microplastics

MDPI

Article

Microplastic Aerosol Contamination in Porto (Portugal)

Yuliya Logvina [1,2], Diogo Silva Moreira [1,2], Rui Pedro Moreira Santos [1,2], Inês Filipa Neves [1,2], Helena Ribeiro [2,3], Luís Pinto da Silva [1,2] and Joaquim Esteves da Silva [1,2,*]

[1] Chemistry Research Unit (CIQUP), Institute of Molecular Sciences (IMS)—DGAOT, Faculty of Sciences, University of Porto (FCUP), Rua do Campo Alegre 697, 4169-007 Porto, Portugal; up201407073@edu.fc.up.pt (Y.L.); diogomoreira09871@gmail.com (D.S.M.); up201608495@edu.fc.up.pt (R.P.M.S.); up202004585@edu.fc.up.pt (I.F.N.); luis.silva@fc.up.pt (L.P.d.S.)
[2] Department of Geosciences, Environment and Spatial Plannings, Faculty of Sciences, University of Porto, 4099-002 Porto, Portugal; helena.ribeiro@fc.up.pt
[3] Earth Sciences Institute (ICT), Pole of the Faculty of Sciences, University of Porto, 4099-002 Porto, Portugal
* Correspondence: jcsilva@fc.up.pt; Tel.: +351-220-402-569

Abstract: Microplastic pollution, particularly particles smaller than 5 mm, poses significant environmental and health risks due to their potential for inhalation and long-range transport. This study provides the first long-term assessment of airborne microplastics and fibers in Porto, Portugal, over 18 months (September 2022 to March 2024). Bi-weekly samples were collected using a Microplastic Collector NILU, which were size-fractionated into five categories (>125 µm, 125–63 µm, 63–25 µm, 25–12 µm, and 12–1.2 µm) and quantified via optical microscopy. Microplastic concentrations ranged from 26 to 1484 MPs/day/m^2, while fiber concentrations varied from 14 to 646 fibers/day/m^2. With a focus on the 12–1.2 µm size range due to their classifications as PM_{10} and $PM_{2.5}$, the highest microplastic concentrations were 164 MPs/day/m^2 (12–1.2 µm) and 534 MPs/day/m^2 (25–12 µm). Recovery rates varied among polymers, with PP, PE-HD, and ABS showing high accuracy (75.9%) and PES significantly lower (26.5%). This study highlights the significant temporal variability in airborne microplastic and fiber pollution, correlations with meteorological parameters, and the need for ongoing monitoring and targeted mitigation strategies to address associated health risks.

Keywords: microplastics; MPs; quantification; air; atmosphere; aerosols; monitoring; sampling procedure; size fractionation procedure; polymer recovery rate

check for updates

Citation: Logvina, Y.; Moreira, D.S.; Santos, R.P.M.; Neves, I.F.; Ribeiro, H.; Pinto da Silva, L.; Esteves da Silva, J. Microplastic Aerosol Contamination in Porto (Portugal). *Microplastics* **2024**, *3*, 696–716. https://doi.org/10.3390/microplastics3040043

Academic Editor: Nicolas Kalogerakis

Received: 3 September 2024
Revised: 8 November 2024
Accepted: 15 November 2024
Published: 20 November 2024

Copyright: © 2024 by the authors. Licensee MDPI, Basel, Switzerland. This article is an open access article distributed under the terms and conditions of the Creative Commons Attribution (CC BY) license (https://creativecommons.org/licenses/by/4.0/).

1. Introduction

Initially investigated in marine ecosystems, microplastic pollution is now recognized as a concerning issue in terrestrial and atmospheric environments. Airborne microplastics (MPs), defined as particles smaller than 5 mm suspended in the air by the European Chemicals Agency (ECHA), have drawn increasing attention due to their potential long-range transport and inhalation by organisms, including humans.

Microplastic contamination in terrestrial environments arises predominantly from landfills, agricultural activities, sewage systems, and transportation. These contaminants migrate within soils, groundwater, and even the atmosphere, posing risks to ecosystems and human health through various environmental pathways [1]. As an emerging concern, airborne microplastics impact both outdoor and indoor environments. While outdoor sources include tire wear, road dust, and sea spray, indoor sources encompass synthetic clothing abrasion and mechanical dryers, highlighting diverse emission sources affecting human exposure and environmental health [2]. Airborne microplastics show diverse concentrations across environments: outdoor air ranging from <1 to >1000 microplastics per cubic meter; indoor air up to 1583 microplastics per cubic meter; and with outdoor/indoor dustfall concentrations reaching up to 1357 and 19,600 microplastics per square meter daily, respectively, and indicate a high exposure potential with PET, PE, and PP identified as the dominant polymers across both environments [3].

The European Union (EU) and the United States of America (USA) have initiated measures to address the growing problem of microplastics in the environment. The EU has been addressing microplastic contamination, and on 25 September 2023, the European Commission published a regulation [4] implementing restrictions on intentionally added microplastics under the REACH Regulation 1907/2006 [5], including a ban on loose glitter and microbeads. Furthermore, on May 12 2021, it adopted the *EU Action Plan: Towards Zero Pollution for Air, Water, and Soil* [6]. This plan aims for a toxic-free environment by 2050, with key targets for 2030 including reducing plastic litter at sea by 50% and decreasing microplastics released into the environment by 30%.

USA legislative efforts have also been focused on reducing microplastic pollution. The Environmental Protection Agency (EPA) and the National Oceanic and Atmospheric Administration (NOAA) have played pivotal roles in these initiatives. The Microbead-Free Waters Act of 2015 [7] marked a significant step by banning the manufacturing and sale of rinse-off cosmetics containing plastic microbeads. NOAA's Marine Debris Program, initiated in 2015 and expanded in 2018, has included research and action plans targeting microplastic pollution in marine environments [8]. Legislative actions continued with the *Save Our Seas 2.0 Act* in 2020 [9], which enhanced efforts to combat marine debris, including microplastics, through improved waste management and international cooperation. More recently, the proposed *Break Free From Plastic Pollution Act of 2021* [10] aimed to address plastic pollution comprehensively, including measures like extended producer responsibility and improved recycling systems. These efforts highlight the global recognition of microplastics as a pressing environmental challenge and the need for continued action to mitigate their impact on ecosystems and human health.

However, regulations are still in the initial stages of development. For atmospheric microplastics, there are currently no standardized methods for sampling, sample preparation, or analysis techniques. Unlike microplastics in water or food, which have seen some progress in standardized protocols, atmospheric microplastic studies lack commonly accepted methodologies, making it challenging to compare findings across different studies. This absence of standardization makes it difficult to maintain consistency in monitoring efforts and limits accurate assessments of exposure risks, environmental impact, and potential health implications. Advancing standardized procedures will be essential for achieving reliable, comparable data on microplastic presence in the atmosphere and its potential impacts.

Research conducted during the last few years highlights new investigations on the sources, distribution, and impacts of airborne microplastics. Studies have identified diverse sources contributing to airborne microplastic pollution, including abrasion of synthetic textiles [11], tire wear [12,13], nail salons [14], the degradation of plastic debris, and atmospheric fallout from plastic waste incineration [15]. These sources vary in their contributions based on geographic location, urbanization levels, and environmental conditions.

Similarly, a recent study has highlighted the seasonal variability in airborne microplastic concentrations, with higher levels observed during increased human activity and atmospheric turbulence [16]. The transport and fate of airborne microplastics are influenced by atmospheric dynamics such as wind patterns and precipitation events [17–19]. Furthermore, the long-distance atmospheric transport of microplastic fibers is influenced by their shapes [20]. Released as airborne microplastics/fibers, these synthetic particles can undergo physical and chemical transformations, potentially adsorbing pollutants and microorganisms and concentrating them in the environment [21].

In the studies reviewed in [22], where various passive sampling methods for airborne microplastics and sample preparation techniques were used, most of them did not utilize standardized capture equipment and lacked sample size fractionation, only occasionally separating larger particulate matter from smaller fractions. In contrast, our study employs a long-term capture strategy over two years, incorporating sample size fractionation ranging from 5 mm to 1.2 μm and utilizing a standardized passive collector. This approach ensures more robust and representative data collection that can be compared with future studies

within each specified size fraction or in total. With this approach, we aimed to further contribute to addressing gaps in both the sampling duration and methodology. Also, we provide, for the first time, the long-term levels and distribution of airborne microplastics in Porto, Portugal, helping to evaluate the extent of this problem for future consideration in potential human health risks and exploring mitigation and monitoring strategies to face the escalating microplastic contamination.

2. Materials and Methods

2.1. Sample Collection

Collecting campaigns for air microplastics were conducted for almost two years, from September 2022 to March 2024. Published procedures were adopted for a passive collection of aerosol microplastic samples and sample preparation [22]. A Microplastic Collector from Innovation NILU AS, designed according to the principles and recommendations outlined in project for ISO standard for particulate deposition collectors, was used for this purpose. The collector was designed to avoid cross-contamination. The sampler was placed in the garden of the Faculty of Sciences of the University of Porto (41.151629, −8.637068), 2.30 m above ground. Cumulative samples were collected every 14 days, transferred from the collector to a dark-glass vial using deionized water and an inox funnel with a 5-millimeter mesh, and stored in the fridge for future sample processing.

Meteorological data were collected using a Campbell Scientific CR200Series meteorological station equipped with sensors to measure various atmospheric parameters. The station was positioned on the roof of the Faculty of Sciences (FC3) of the University of Porto close to the sample collecting place to ensure a representative sampling of regional weather conditions. Continuous monitoring included the following: temperature, humidity, precipitation, wind speed, and direction. Data were logged at 10-min intervals and stored in a database for subsequent analysis.

2.2. Sample Preparation

The following equipment and materials were utilized for sample preparation: A vacuum pump LABOPORT® No. 96 (KNF, Schenkon, Switzerland) aided in passing the sample through the filtration system into a flask. Three stainless steel sieves (HAVER & BOECKER, Oelde, Germany) with diameters of 5 cm and mesh sizes of 125 µm, 63 µm, and 25 µm were used for particle fractionation of the collected aqueous samples. A sonicator (VWR®, Radnor, PA, USA) was used to disperse aggregates in the aqueous samples and for cleaning the materials. An oven (Heraeus Instruments, Hanau, Germany) was used to digest organic matter in treated samples. A glass filtration system (Normax, Marine Grande, Portugal) suitable for various filtration membranes was employed. Cellulose nitrate (CN) filtration membranes with pore sizes of 12 µm and 1.2 µm from Whatman® Cytiva (Maidstone, UK) and CHMLAB Group (Barcelona, Spain) were used. Hydrogen peroxide (H_2O_2) 30% (diluted to 15%) from Carlo Erba Reagents (DasitGroup, Cornaredo, Itália) was used to degrade organic matter in samples. An optical microscope VisiScope® 534, (VWR®, Radnor, PA, USA) with transmitted light and 10×, 20×, and 40× objectives was used to quantify microplastics and fibers.

The sample preparation procedure, as described in Section 2.1, was adopted from a previous study [22] and started with a size-fractionation step using inox sieves and a glass filtration system with membrane filters (Figure 1). Five size fractions for each sample were obtained: 5 mm–125 µm, 125–63 µm, 63–25 µm, 25–12 µm, and 12–1.2 µm. Before fractionation, samples were homogenized. The entire sample from the dark-glass vial was filtered and the vial and containers were washed three times with deionized water to ensure maximum sample extraction. As a first step, for sieving, a vacuum suction was applied using a vacuum pump. The next step included the filtering of the remaining liquid samples through 12 µm and 1.2 µm filter membranes—corresponding to particle size fractions of 25–12 µm and 12–1.2 µm—using the glass filtration system.

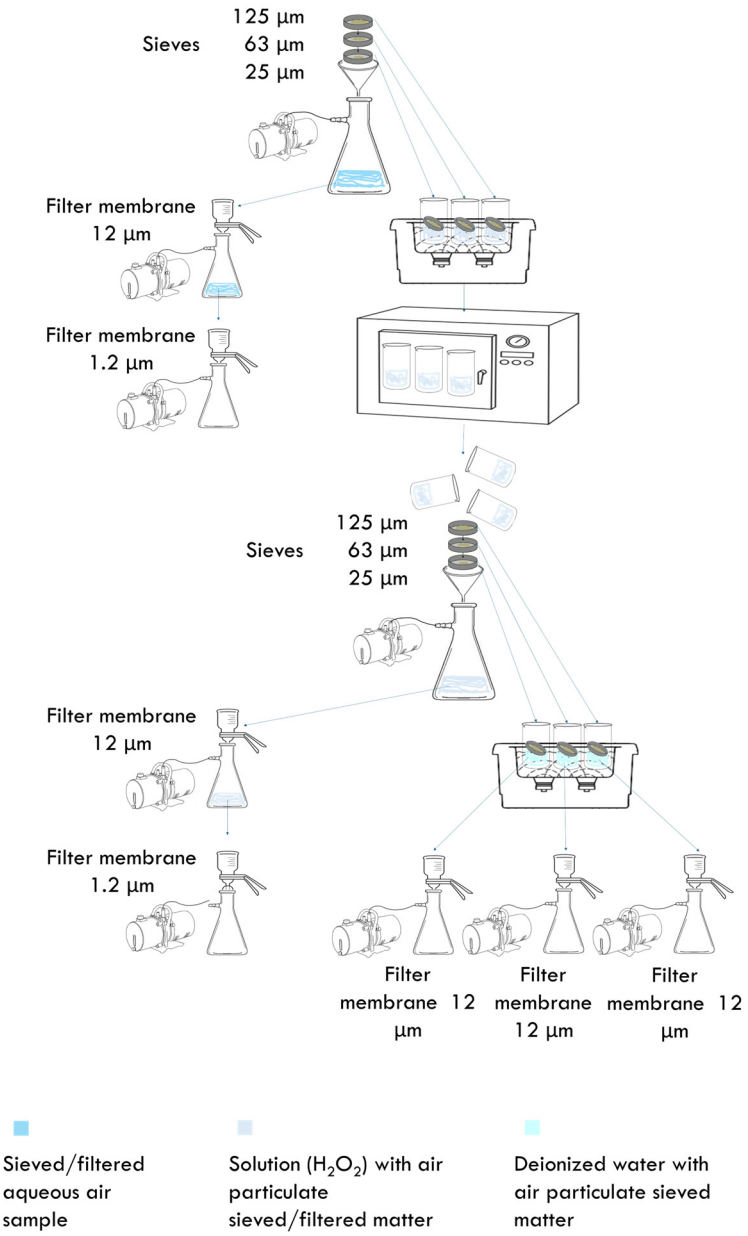


Figure 1. Scheme for the sample preparation process using sieving and filtration.

Each sieve (125 µm, 63 µm, and 25 µm) with the material retained there was placed in individual 250 mL beakers with H_2O_2 (15%) and sonicated for a few seconds. After sonication, the sieves were removed, washed in the beakers that were subsequently covered with aluminum foil, and placed in an oven at 50 °C for 12 h for organic matter digestion. This step is essential for visualizing microplastics under the microscope, as smaller microplastics adhere to organic matter. Afterward, the organic matter digestion solution (H_2O_2) containing particulate matter from the beakers was sieved and filtrated again, as described above. Separated matter in the sieves was detached in the deionized water and filtered through 12-micrometer membrane filters using a glass filtration system yielding fractions >125 µm, 125–63 µm, and 63–25 µm. The remaining water sample was filtered again through 12 µm and 1.2 µm membranes to capture small, detached particles. During each filtration step, three rounds of water–throwing–washing were conducted to ensure total sample extraction. Filters were stored separately in aluminum foil until analysis.

2.3. Control Sample and Recovery Rate Determination

Since the filtration of all samples was conducted in three sets, to account for lab contamination during each set of filtrations, three control tests with deionized water were conducted using the same filtration procedure, quantifying microplastics similarly to actual samples. Average control values were subtracted from the sample values of the according set.

For recovery rate (RR) determination, four types of polymers were used as follows: polypropylene (PP), high-density polyethylene (PE-HD), acrylonitrile butadiene styrene (ABS), and polyester (PES). Polymers were sourced from various items: PP (bright green) from water sport bottle caps; PE-HD (magenta) from lab-reagent bottle caps; ABS (violet) from LEGO pieces; and PES from fluorescent yellow-green cords. PP, PE-HD, and ABS represent synthetic polymers with particle shapes, while PES represents a fibrous polymer. Polyamides, such as nylon, are also prevalent in various environments; however, we chose to focus on polyester as the primary fibrous polymer for this study to avoid overloading the sample with multiple fibrous polymer types. This decision was made to ensure clear identification and analysis of key materials while maintaining the integrity of the sample. PP, PE-HD, and ABS were ground using a stainless-steel coffee grinder, while PES fibers were cut into smaller pieces using scissors. Ground PP, PE-HD, and ABS particles were added to water and filtered through the sieves to obtain polymer particles for each size fraction. It was observed that during grinding, smaller polymer particles became more filamentous. Only polymer particles larger than 125 µm were selected due to their microplastic particle morphology. Thirty microplastic particles of each polymer (PP, PE-HD, and ABS) were placed in three sampling flasks from the same sampling period to ensure matrix complexity. The PES, a cut fibrous polymer, was mixed with water, filtered through sieves, and then through filter membranes for quantification. For PES, fibrous particles in the size-fraction intervals >125 µm and 125–63 µm had lengths $\geq$4 times their width, while those in the 63–25 µm and 25–12 µm intervals had lengths $\leq$3 times their width. In each flask, over 200 larger PES fibers (lengths $\geq$4 times their width) and more than 50 smaller PES fibers (lengths $\leq$3 times their width) were added, previously counted on membrane filters. Aqueous samples with added polymers were filtered similarly to the previously described procedure in Section 2.2, allowing some polymers to escape to verify recovery rates. Quantification was performed by considering the distinct colors and forms to distinguish them from regular samples (Table S1).

2.4. Microplastic Quantification

Optical microscopy with transmitted light was used to quantify MPs and fibers present in the filter membranes for each of the five size fractions: >125 µm, 125–63 µm, 63–25 µm, 25–12 µm, and 12–1.2 µm (Table S2). Given the limitations of this technique in identifying microplastics, where color differentiation can be uncertain and potentially confused with other materials, bright colors not typically found in nature at this range—red, blue, green, yellow, orange, purple, and pink—were selected for counting microplastics. Both colored and colorless fibers were quantified.

The sample from 29 September 2022 to 26 October 2022, which covered 27 days, was divided into two parts (29 September 2022a and 29 September 2022b; 26 October 2022a and 26 October 2022b) to facilitate comparisons with the other 14-day samples.

Absolute numbers and percentages of microplastics (MPs) and fibers were calculated for each sample and each fraction. According to studies accepted by the scientific community, the units for microplastics obtained by passive sampling are expressed as MPs per day and per square meter (MPs/day/m^2). While "particles" could indeed represent all types of particles, including mineral or organic, such as carbon soot, in the specific context of air microplastic research the abbreviation "MPs" is used to refer to microplastic particles (lengths $\leq$3 times their width), while "Fbs" denotes fibers (lengths $\geq$3 times their width), allowing for clear differentiation between particle types. Expressing the results as MPs/day/m^2 aligns with passive sampling methods, where deposition rates are typically

reported in this manner due to the nature of collection, which relies on gravity-driven processes such as dry fallout or wet precipitation. In contrast, active sampling methods, where air is suctioned through a filter using a pump with a known flow rate (L/min), generally report results in MPs/m^3. Therefore, the number of MPs per day and per square meter (MPs/day/m^2) was determined for the total size fractions (5 mm–1.2 µm) and for the two smallest size fractions (25–12 µm and 12–1.2 µm); the number of fibers per day and per square meter (fibers/day/m^2) was determined for just the total size fractions (5 mm–1.2 µm).

The meteorological data and microplastic/fiber concentrations (MPs/day/m^2 and fibers/day/m^2) were analyzed to identify any significant correlations or patterns, with wind roses used to visualize the wind directions. Statistical tests included Spearman's Rank Correlation, and Principal Component Analysis (PCA) was performed to determine the relationship between meteorological conditions and the concentration of airborne microplastics and fibers. All calculations were performed in Excel, including data preparation and adjustments. Statistical analyses, such as Spearman's rank correlation coefficients for the wind rose and microplastics, were also conducted in Excel for Microsoft 365, Version 2410. PCA was carried out using Origin 9.0 software.

The overall average recovery rate of polymers was not applied as a correction factor in calculating the collected MPs or fibers in the samples. This decision was made to avoid potential errors as the recovery rate analysis was only conducted for microplastic particles larger than 125 µm, which may differ from smaller microplastic polymer particles. Additionally, the recovery rate was only verified for one type of fiber, polyester, and may not accurately represent other types of fibers.

3. Results

3.1. Recovery Rates for Plastic Polymers

The recovery rates for four types of polymers, PP, PE-HD, ABS, and PES, were evaluated through a series of three separate trials for the same period sample. Table 1 summarizes the recovery rates during the filtration process. The recovery rates were assessed across the size fraction >125 µm for PP, PE-HD, and ABS, considered particulate microplastic, and across >63 µm and 63–12 µm size fractions for the PES, fibrous microplastic. The average recovery rates for each polymer and the overall average are also provided to evaluate the efficiency of the filtration process.

Table 1. Recovery rates for four plastic polymers during the sample filtration process.

Polymer	Polymer Morphology	Fraction (µm)	RRs %/Washing			Average RRs %	Overall Average RRs %
			1st	2nd	3rd		
PP	particulate	>125	60.0	86.7	80.0	75.6	75.9
PE-HD			90.0	70.0	70.0	76.7	
ABS			70.0	63.3	93.3	75.6	
PES	fibrous	>63	52.6	25.5	26.0	34.7	26.5
		63–12	24.2	14.0	16.4	18.2	

RR—recovery rate; PP—polypropylene; PE-HD—polypropylene high density; ABS—acrylonitrile butadiene styrene; PES—polyester.

The recovery rates for the polymers varied across the trials, reflecting the effectiveness of the filtration process in capturing different types of microplastics. PP exhibited high recovery rates in the second and third trials (86.7% and 80.0%), while the first trial's recorded recovery was lower (60.0%), resulting in an average recovery rate of 75.6%. PE-HD showed consistent recovery rates across the trials (90%, 70%, and 70%), with an average recovery rate of 76.7%. ABS exhibited a wide range of recovery rates in the >125 µm fraction, with the third trial showing the highest recovery rates (93.3%); the first and the second trials had lower recovery (70.0% and 63.3%), resulting in an average recovery rate of 75.6% for ABS, which is equal to the average recovery rate of PP. PES had lower recovery rates compared

to the particulate polymers. The >63 µm fraction had recovery rates of 52.6%, 25.5%, and 26.0%, averaging 34.7%. The 63–12 µm fraction had recovery rates of 24.2%, 14.0%, and 16.4%, averaging 18.2%. These results indicate lower recovery efficiency for PES compared with the other polymers, in both of the size fractions analyzed, which may be due to the filamentous nature of PES that is more challenging in the filtration process.

3.2. Quantification of MPs and Fibers in the Air

Results of the quantification of MPs and fibers by optical microscopy are represented in Figure 2 and show the distribution of total microplastics and fibers in the samples collected from September 2022 to March 2024. The number of microplastics collected varied considerably over this period, with the highest count recorded on 26 April 2023 (653 MPs) and the lowest on 7 December 2022 (11 MPs). Similarly, fiber counts showed variability along the study period, with the highest number recorded on 10 May 2023 (284 fibers), and the lowest on 7 December 2022 (6 fibers). Several notable peaks in microplastic counts were observed, including 387 MP particles on 10 May 2023, and 329 MP particles on 24 May 2023. Fiber counts also displayed peaks on these dates and generally follow the same trends, with the most fibers collected on 10 May 2023 (284 fibers), and on 24 May 2023 (220 fibers).

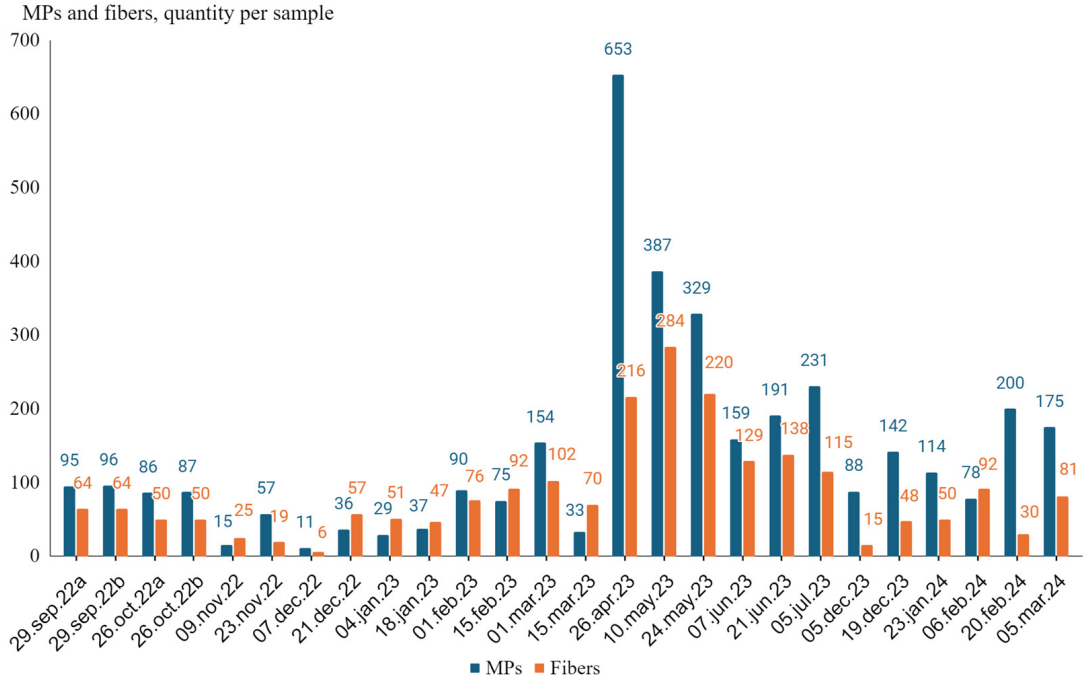


Figure 2. Total absolute number of MPs and fibers in each collected sample.

When viewed as percentages, the relative proportions of microplastic to fibers also showed notable fluctuations (Figure 3). Microplastic particles ranged between 32% and 87% of the total number of microplastics and fibers, while fibers ranged from 13% to 68%. Notable peaks in microplastic particle counts were observed in April and May 2023 but the highest percentage (87%) was recorded on 20 February 2024. The highest fiber percentage (68%) occurred on 15 March 2023, indicating the existence of periods where fibers were more prevalent than microplastics.

The data for the fiber counts by size fraction across the various samples from September 2022 to March 2024 show distinct distribution patterns among different size ranges (Figure 4). Fibers were classified into five size fractions: >125 µm, 125–63 µm, 63–25 µm, 25–12 µm, and 12–1.2 µm. The majority of fibers were found in the 25–12 µm and 12–1.2 µm size fractions, with considerably fewer fibers in the bigger size fractions (>125 µm and 125–63 µm). For the >125 µm size fraction, fiber counts were generally low, with notable peaks on 26 April 2023 (65 fibers) and 10 May 2023 (50 fibers). Many samples recorded zero

fibers in this size range. Similarly, the 125–63 µm size fraction also showed low counts with occasional peaks, such as 10 May 2023 (38 fibers). The 63–25 µm size fraction had moderate fiber counts with peaks between 1 February 2023 and 5 July 2023 (65–74 fibers). The 25–12 µm size fraction consistently showed higher counts, particularly notable on 10 May 2023 (118 fibers) and 24 May 2023 (82 fibers). Lastly, the 12–1.2 µm size fraction was the most consistently populated, with high counts across multiple dates, such as 21 December 2022 (57 fibers), and the lowest on 7 December 2022 (6 fibers).

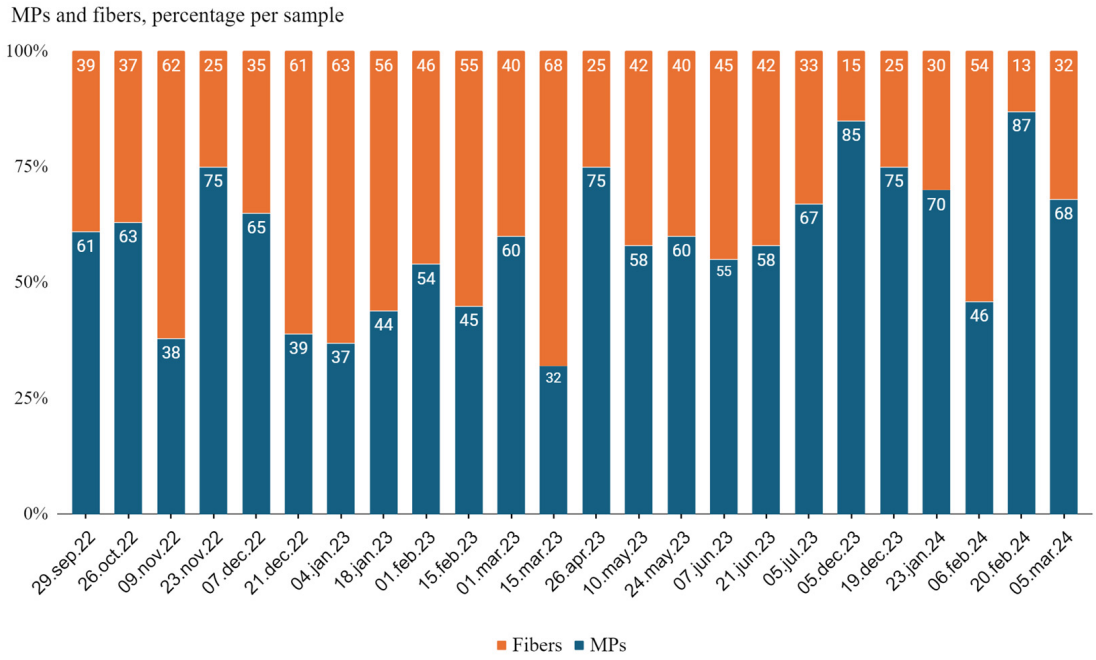


Figure 3. Percentage of total MPs vs. fibers in each collected sample.

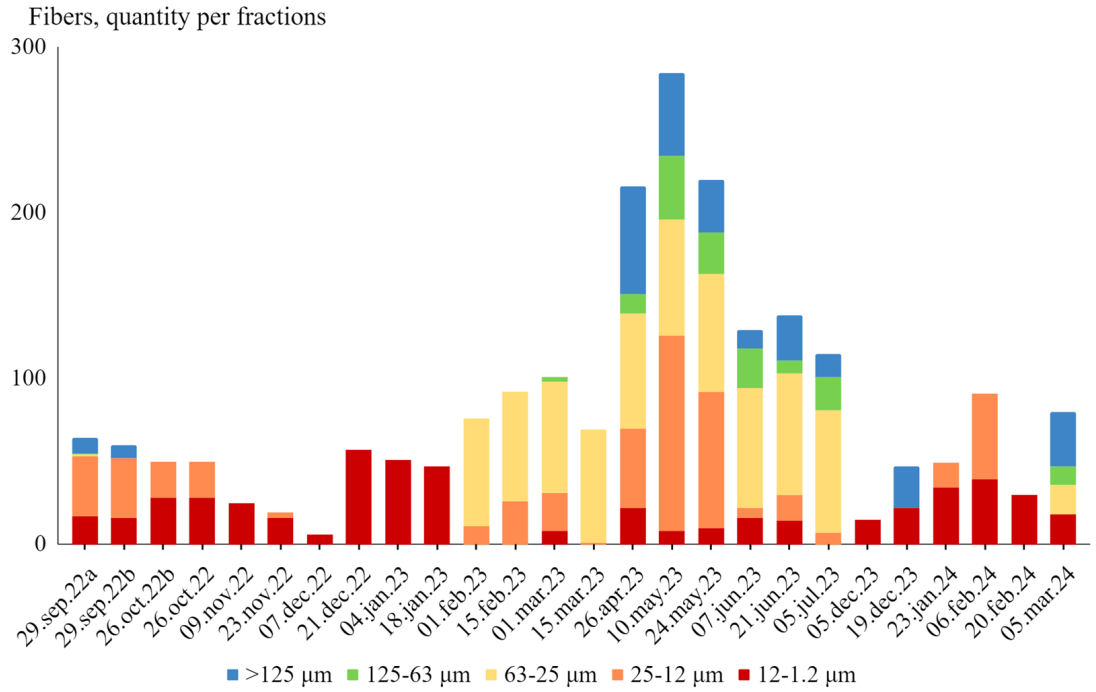


Figure 4. Fibers counted by the size fractions in each collected sample.

Evaluating the percentage of fibers within the total synthetic polymer particles in each sample (Figure 3), we observed that in three pairs of samples (9 November–23 November

2022; 15 March–26 April 2023; and 6 February–20 February 2024), there was a pronounced decrease in fiber percentage in each subsequent sample. Comparing these percentages with the counts of microplastic and fiber particles (Figure 2) and detailing fiber counts by size fraction (Figure 4) we see that a decrease in fiber percentage is associated either with an increase in microplastic counts or a decrease in fiber counts—either within specific fiber size fractions or across the total fiber particle count—and vice versa.

In particular, for consecutive samples collected on 6 February 2024 and 20 February 2024, the microplastic count in the 20 February sample was approximately four times higher than in the 6 February sample, while fiber counts were reduced by about 1.5 times. Meteorological data (Table S3) from this period reveal an exceptional condition: unlike other collection periods, there was no precipitation during the sampling of 6 February 2024. Furthermore, in the subsequent sampling on 20 February 2024, the maximum wind speeds increased to 17 m/s compared to 8 m/s in the previous collection. This suggests that rain may act as a clearing mechanism for microplastics in the atmosphere, potentially lowering fiber proportions when microplastic counts increase, thus making the fiber percentage less pronounced. In another sampling period, comparing samples from 15 March 2023 and 26 April 2023, the microplastic count in the 26 April sample increased by twenty times, while fiber counts were three times higher. A review of meteorological conditions during this period revealed a significant temperature increase from 19 °C to 29 °C, a temperature difference not observed during any other collection period. Notably, this sample also had the highest number of microplastics recorded throughout the entire sampling period, with 653 MPs per day per square meter. For the third set of sample pairs, collected on 9 November 2022 and 23 November 2022, rainfall nearly doubled during the 23 November sampling period, with no notable changes in other meteorological factors. During this time, the number of microplastics increased threefold, while fiber counts decreased by threefold in the 23 November sample, underscoring the observed decrease in fiber counts during rainy periods, as was seen in the sample collected on 20 February 2024.

The analysis of microplastic particle contamination across different size fractions (>125 µm, 125–63 µm, 63–25 µm, 25–12 µm, and 12–1.2 µm) revealed considerable variability and different trends (Figure 5). The data show that the mean of microplastic counts decreases with increasing size fraction, with 17 MPs for >125 µm, 18 MPs for 125–63 µm, 31 MPs for 63–25 µm, 66 MPs for 25–12 µm, except for 12–1.2 µm, with a mean of 21 MPs. These results indicate a higher prevalence of smaller microplastic particles, likely more pervasive due to degradation processes. The variability and presence of outliers suggest localized dates of high contamination, pointing to the influence of specific environmental factors or sources. The absence of outliers in the smallest size fraction (12–1.2 µm) suggests a more uniform distribution of microplastics in this category. For the >125 µm fraction, most data fall from 0 to 61 MPs, with a mean of 17 MPs and one expressive outlier at 114 MPs. This suggests that while most samples contain a moderate number of larger microplastic particles, there are occasional occurrences of considerably high counts, possibly due to localized contamination. The data show a similar trend in the 125–63 µm fraction, with a mean of 18 MPs and a prominent outlier at 75 MPs. This indicates that microplastics in this size range are less prevalent than larger microplastic particles; however, again, localized factors can cause high variability. The 63–25 µm category shows a broader range of microplastic particle counts with a mean of 31 MPs and notable outliers at 98 and 235 MPs. The more substantial number of outliers and higher variability suggest that this size fraction is more susceptible to environmental factors that can lead to spikes in microplastic counts. For the 25–12 µm fraction, the mean count of 66 MPs and an outlier of 235 MPs indicate a higher prevalence of microplastic particles in this size range. This could be because smaller microplastic particles are more likely to be produced and persist in the air, potentially accumulating from various sources. The 12–1.2 µm fraction, with a mean of 21 MPs and no outliers, shows the smallest range of variability. The absence of outliers might suggest a more uniform distribution, constant affluent taxes, and sources of

high microplastic counts in this size range. Generally, there appear to be fluctuations but potentially increasing trends in microplastic concentrations over the sampling period.

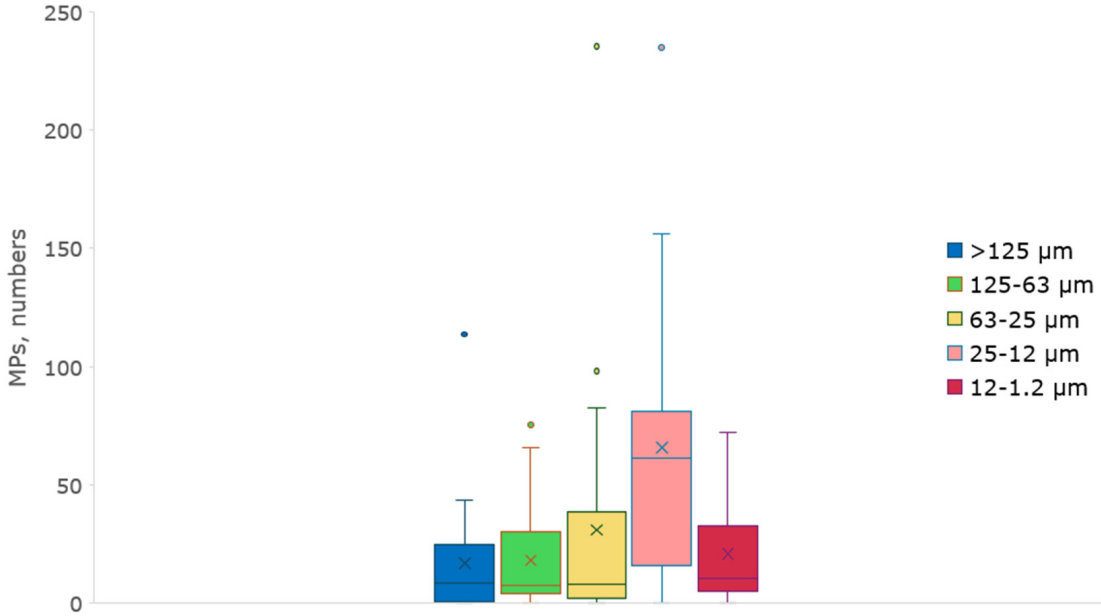


Figure 5. Box plots and outliers of absolute number of MPs in each size fraction across all collected samples.

The box plots in Figure 6 visually represent the distribution of MPs and fibers per day and per square meter across the samples collected from 29 September 2022 to 5 March 2024. The number of MPs/day/m^2 ranges from 26 to 1484, with the mean (329), median (211), quartiles (119 and 407), and outliers (879 and 1484) identified for each time point, revealing trends in microplastic pollution over time. There is notable variation in microplastic concentrations across different sampling dates. For instance, the highest concentration was observed on 26 April 2023 (1484 MPs/day/m^2), while the lowest was on 7 December 2022 (26 MPs/day/m^2). In the previous box-plot analysis (Figure 5), each fraction, excluding the 25–12 µm, exhibits a notable increase toward the upper quartile of the plot. Similarly, we observe this trend in the current box plot depicting MPs per day per square meter for the total fraction across all samples. There is a clear tendency toward higher concentrations over the sampling period, indicating a potential increase in microplastic levels.

The numbers of fibers/day/m^2 range from 14 to 646, with the mean (197), median (150), quartiles (108 and 239), and two outliers (492 and 646). Generally, there appear to be fluctuations but potentially increasing trends in fiber concentrations over the sampling period too.

The counts of MPs/day/m^2 for the total fractions (5 mm–1.2 µm) and each fraction (25–12 µm and 12–1.2 µm) vary considerably over time, specific periodic dates with unusually high MP counts might suggest episodic pollution events, seasonal effects, or other influencing factors (Figure 7).

The counts of microplastics within the two lowest size fractions (25–12 µm and 12–1.2 µm) calculated per day and per meter square (MPs/day/m^2) over the sampling period reveal notable variability in microplastic concentration across both size categories and sampling dates. MPs in the size fraction 25–12 µm are generally more abundant than smaller ones, except for the period from 7 December 2022 to 17 January 2023. Overall, the data do not indicate consistent proportions, trends, or relationships between the different fractions of MPs. The counts of MPs within the total fractions (5 mm–1.2 µm) and each fraction (25–12 µm and 12–1.2 µm) vary independently and do not exhibit a clear pattern when compared to one another. Nevertheless, even with this variability, size fractions 25–12 µm display an increasing trend of represented values.

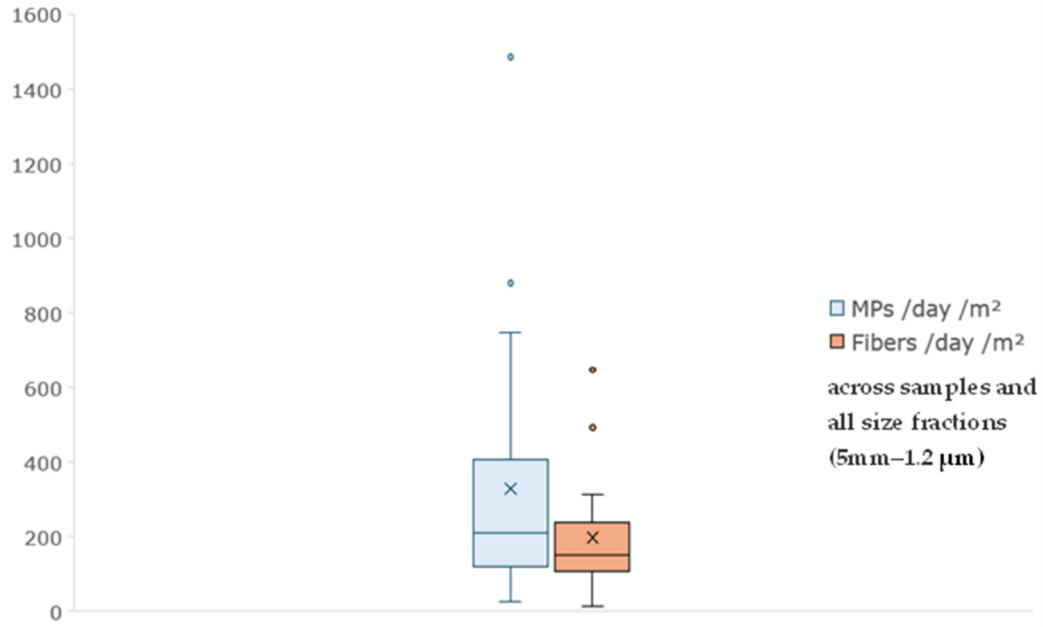


Figure 6. Box plots of number of MPs and fibers per day per square meter (MPs/day/m^2) for total fractions in each collected sample.

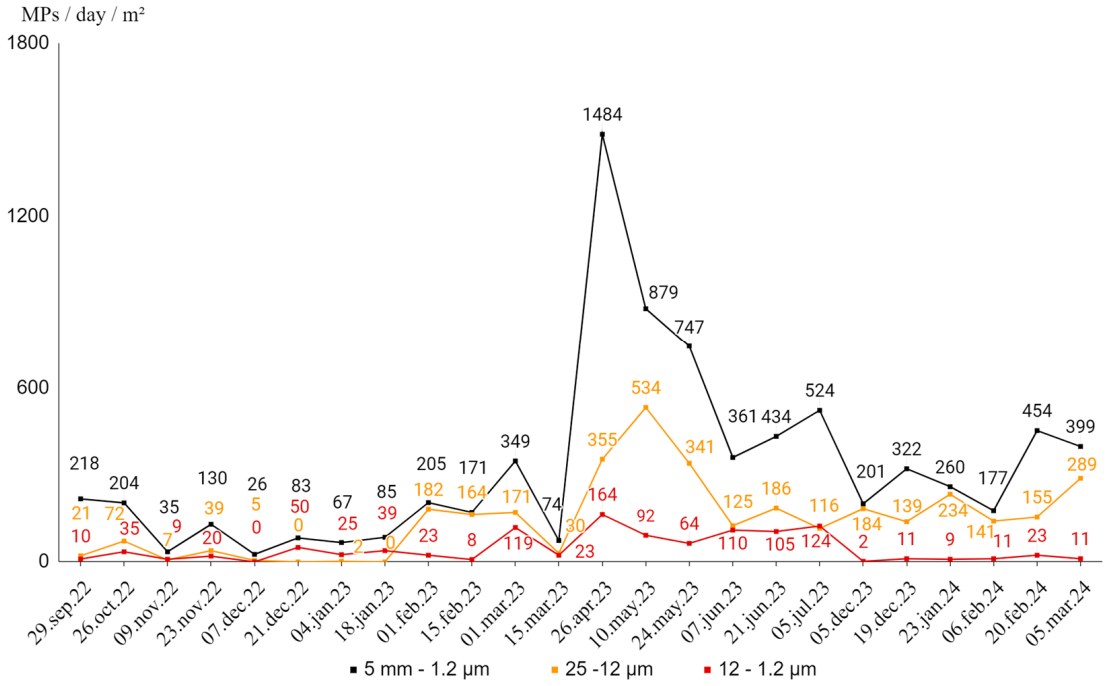


Figure 7. MPs were calculated per day per square meter (MPs/day/m^2) across collected samples and within the two smallest fractions (25–12 µm and 12–1.2 µm), as well as for total of fractions (5 mm–1.2 µm), without applying the recovery rate.

The wind rose data, collected from 29 September 2022 to 5 March 2024, illustrate the distribution and frequency of wind directions over the study period (Figure 8). The observations reveal that the wind predominantly blew from the east (E), south (S), southwest (SW), and north (N) directions. The analysis of predominant wind directions for each sample period from 29 September 2022 to 5 March 2024 revealed distinct patterns (Figure 9). The data indicate that the predominant wind direction varied considerably across the different sampling dates, reflecting the dynamic nature of local meteorological conditions.

Throughout this study, easterly (E) winds were the most frequently predominant direction, especially notable on 15 February 2023 with a maximum count of 273 occurrences. This trend continued with significant instances on 6 February 2024 (245), 7 December 2022 (228), and 1 March 2023 (169). Southern (S) winds were predominant on several occasions with the most significant instance on 26 October 2022 (193) and notable occurrences on 4 January 2023 (139) and 9 November 2022 (114). In contrast, the northern (N) winds were predominantly observed on fewer occasions, including 5 July 2023 (112), 10 May 2023 (76), and 5 March 2024 (66). Moreover, southwestern (SW) winds were primarily dominant on 29 September 2022 with 146 occurrences, on 21 June 2023 with 91 instances, on 23 November 2022 with 87 instances, and on 7 June 2023 with 82 instances. These instances underscore the variability and occasional prominence of S and SW winds in the study area. Interestingly, there were no instances of predominant winds from the southeastern (SE), western (W), or northwestern (NW) directions during the sampling periods, indicating a limited influence from these directions within the observed timeframe. The northeastern (NE) winds were predominant on 24 May 2023, with 120 instances, marking a unique occurrence where NE winds dominated.

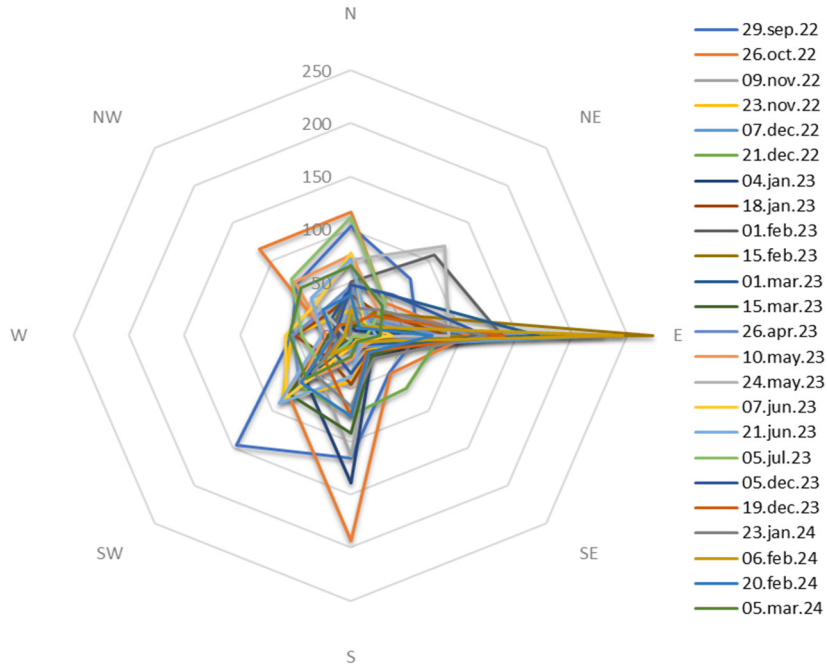


Figure 8. Wind rose schemes projected for winds during sampling period: all winds in absolute frequencies for each collected air sample.

Overall, the data demonstrate that while easterly, southerly, and southwesterly winds were more consistently predominant, there was considerable variability in wind direction, with certain periods experiencing strong influences from the northerly, northwesterly, and northeasterly winds. This variability is crucial for understanding the dispersion patterns of airborne materials, including microplastics and fibers, within the study region.

The analysis of Spearman's rank correlation coefficients (r_s) and associated *p*-values reveals that different wind directions have distinct impacts on the concentration of microplastics and fibers in the environment (5 mm–1.2 µm) (Figure 10). Spearman's rank correlation coefficient ranges from 1 to −1 and measures monotonic relationships rather than strictly linear ones and a low *p*-value ($p < 0.05$) indicates that the correlation is statistically significant. For northwest (NW) and north (N) winds, strong positive correlations were observed between NW and N winds and microplastics per day and per square meter ($MPs/day/m^2$), particularly for the total MP fractions (5 mm–1.2 µm), with correlation coefficients of 0.70 and 0.68, respectively. These correlations are highly significant, with *p*-values of 0.0001 and 0.001, indicating that stronger winds from these directions are associated with

increased levels of MPs. For northeast (NE) winds, moderate positive correlations were found, particularly for the MP fraction 25–12 µm and the total MP fractions (5 mm–1.2 µm) with correlation coefficients of 0.45 and 0.44, respectively. The significance of these relationships is supported by *p*-values of 0.03, suggesting that NE winds may contribute to higher concentrations of these microplastic particles.

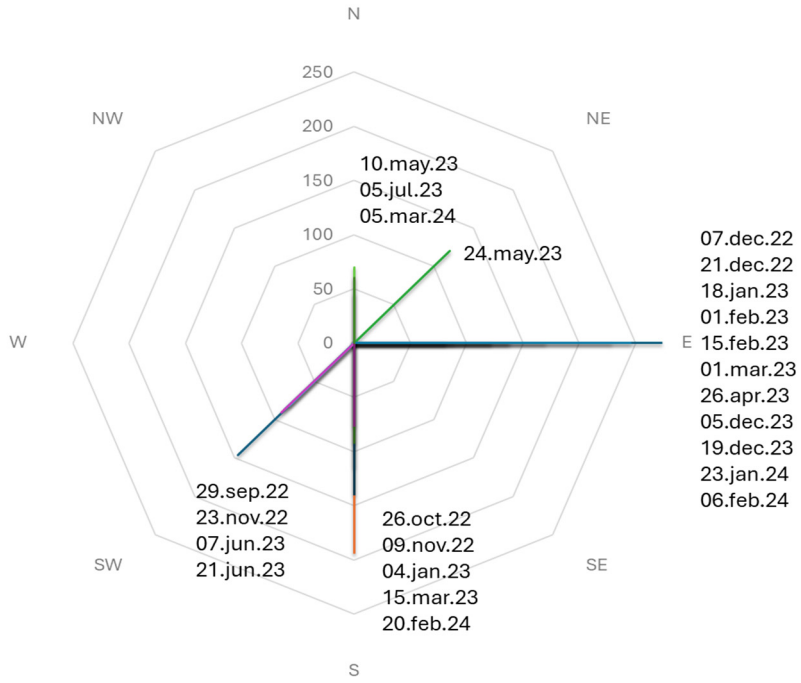


Figure 9. Wind rose schemes projected for winds during sampling period: predominating wind in absolute frequency for each collected air sample.

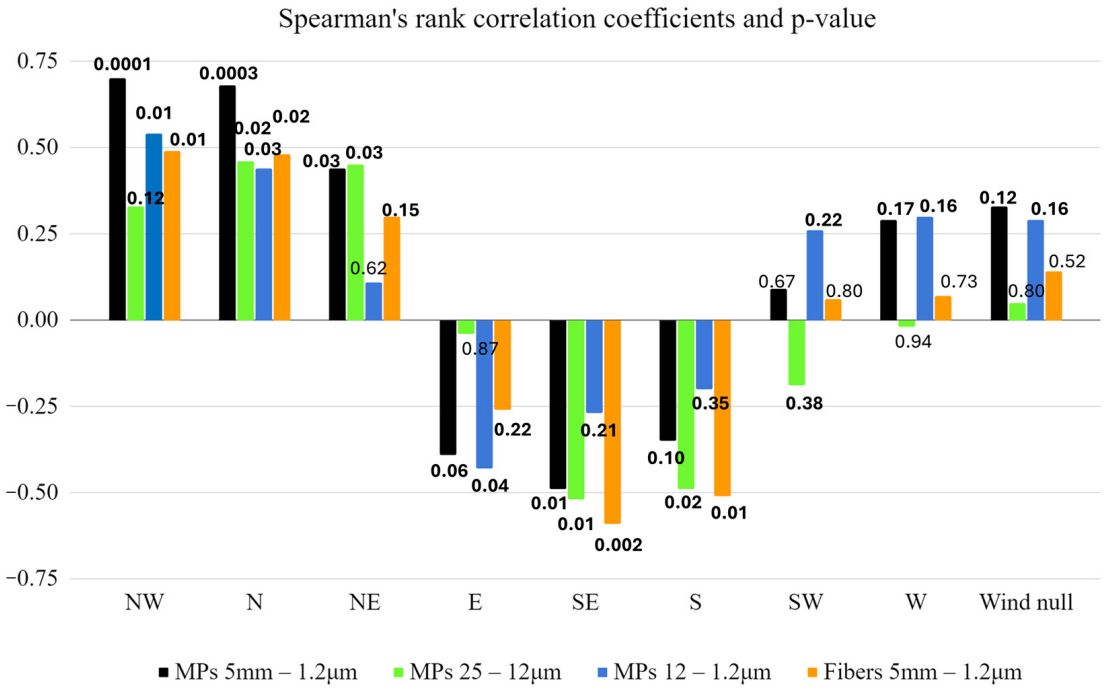


Figure 10. Spearman's rank correlation coefficients with associated probabilities (*p*-values) for different wind directions and size fractions of MPs and fibers.

In contrast, southern (S) and southeast (SE) winds tend to have negative correlations with most MP particle sizes and fibers. The strongest negative correlations were found with fibers in the 5 mm–1.2 μm range (−0.51 and −0.59, respectively), with significant *p*-values of 0.01 and 0.002. This negative correlation suggests a moderate inverse relationship between these two variables, indicating that stronger winds from the S and SE directions are likely to reduce the concentrations of fibers and MPs. Eastern (E) winds also showed negative correlations, particularly with the MP fraction 12–1.2 μm (−0.43) and the total MP fractions 5 mm–1.2 μm (−0.39); however, the *p*-values are 0.04 and 0.06, suggesting a potential, less pronounced, inverse relationship between E winds and microplastic concentrations. Winds from the west (W), southwest (SW), and periods with no significant wind (null) generally showed non-significant correlations (*p*-values above 0.05), suggesting that these directions may have a less consistent influence on microplastic levels.

These findings suggest that wind direction plays a crucial role in influencing the distribution of microplastics and fibers in the environment. Northern and northeastern winds generally increase microplastic/fiber particle concentrations, while southern and eastern winds may contribute to their reduction.

During the analysis of the relationship between meteorological factors and the concentration of microplastics, an assessment was conducted to determine the presence of linearity between the independent variables (meteorological factors) and the dependent variable (MPs). Despite thorough evaluation, no significant linear relationships were identified. Therefore, a Principal Component Analysis (PCA) was employed as it does not require linearity and is effective in reducing dimensionality by identifying the principal components that explain the most variance in the data. This technique allowed for the exploration of complex, non-linear relationships between the meteorological factors and microplastic concentrations, providing a more comprehensive understanding of the underlying patterns in the data.

PCA was employed to investigate the relationships between MP (5 mm–1.2 μm) concentrations (MPs/day/m^2) and various meteorological factors related to wind, temperature, relative humidity, and precipitation (Table S3). The analysis identified key components that explain the majority of the variance in the dataset, offering insights into the impact of different environmental variables on microplastic levels (Figure 11). The PCA revealed seventeen principal components, with the first three components explaining 82.84% of the total data variance (41.54%, 26.15%, and 15.16%, respectively), indicating that they capture the most significant patterns in the data. The first principal component (PC1) is strongly associated with wind speed and precipitation variables, as evidenced by high positive factor loadings (Table S4) such as "Wind max", "Precipitation tot", and "Precipitation occur". These results suggest that PC1 reflects the combined influence of wind speed and occurrence of precipitation on microplastic concentrations, where high wind or intense precipitation might lead to the dispersion or removal of airborne microplastics. Conversely, temperature-related variables like "Temperature avr max" and "Temperature avr avr" presented negative loadings, indicating an inverse relationship with PC1. The second principal component (PC2) was dominated by temperature and humidity factors, with substantial positive loadings for "Temperature avr min", "Temperature avr avr", and "Humidity avr max". PC3 primarily reflects the variations in wind speed, with high positive loadings for "Wind avr", "Wind max", and "Wind avr max". These previous two components point toward a potential lower seasonal influence on microplastic distributions driven by these meteorological variables. The highest loading in PC4 is for MPs/day/m^2, suggesting that this component may primarily represent the variance in microplastic counts directly. High positive loadings in PC4 for "Humidity min" indicate that humidity levels, particularly "Humidity min", could correlate strongly with microplastic presence in the samples. This suggests that during low-humidity periods, there might be more accumulation of airborne microplastics.

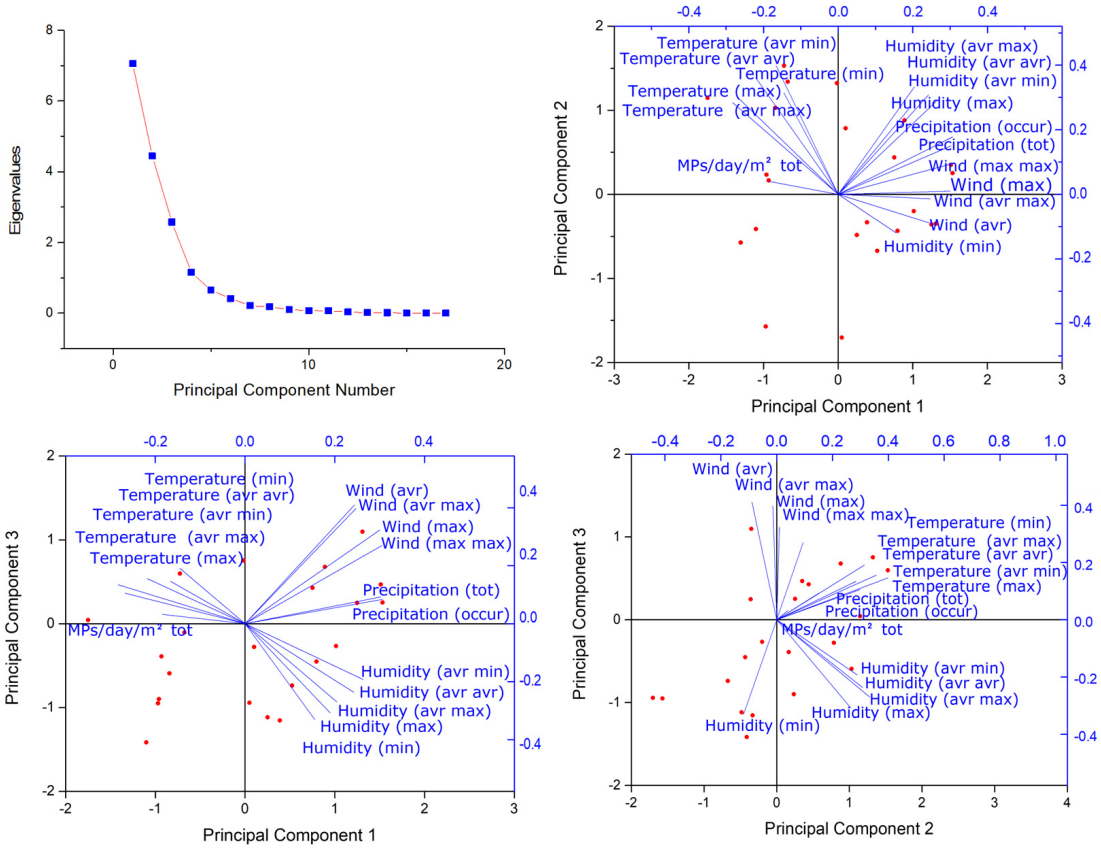


Figure 11. Principal component analysis of microplastic concentrations (MPs/day/m^2) for total of fractions (5 mm–1.2 µm) and meteorological factors (16 components: wind, precipitation, temperature, humidity). Screen plot for Eigenvalues and biplot for principal components (PC1, PC2, and PC3) and observed values.

These findings provide a nuanced understanding of the complex interplay between meteorological variables and microplastic concentrations, offering a foundation for further exploration of their environmental impact.

While the application of statistical analysis to our data has been valuable in uncovering patterns in microplastic distribution, the results indicate that meteorological factors alone may not fully account for certain environmental and human influences. For instance, the drastic increase in the number of MPs observed in the sample collected on 26 April 2023 (Figure 2) may partly be explained by a significant temperature increase from 19 °C to 29 °C (a temperature difference not observed during any other collection period). Additionally, this type of anomaly in microplastic and fiber counts could be influenced by various other factors beyond weather conditions, corroborated by the PCA analysis where the microplastic variable has the highest score at PC4 (0.757356) (Table S4). This includes factors such as nearby urban construction projects, increased traffic emissions, increased industrial activity in factories or facilities, roadworks or infrastructure projects, waste management disruptions—such as increased waste burning or improper disposal—and other localized human activities. Furthermore, the interaction of multiple variables—such as wind direction changes coinciding with construction dust or unusual atmospheric conditions—might have contributed to the spike. It appears that atmospheric microplastic levels are influenced by a complex combination of factors, including meteorological variables and other environmental conditions, some of which remain unmeasured or poorly understood. While this study did not include all such variables due to gaps in our current understanding, it is possible that these unmeasured factors play a significant role in microplastic distribution too. These combined factors may not be immediately visible in the data but could be more apparent through a broader examination of the environmental and anthropogenic

influences around the sampling area. The fluctuations observed in microplastic and fiber levels suggest that these interactions are dynamic, and such an approach is crucial to fully grasp the drivers behind microplastic distribution in the atmosphere.

4. Discussion

In this study, we reported airborne microplastic particles and fibers present in air samples in five size fractions (5 mm–125 µm, 125–63 µm, 63–25 µm, 25–12 µm, and 12–1.2 µm). This allowed us to calculate the number of microplastics or fibers per day and per square meter (MPs/day/m^2) for the entire sample and each size fraction, unlike several reported cases that do not perform this fractionation [22], representing microplastics or fibers for the entire sample without size fractionation. Therefore, some of our results cannot be directly compared to those from other studies.

Comparing results of air microplastic contamination is highly subjective due to differences in sample capture methods (active air suction and passive deposition, which can be dry, wet, or both). Even with the same capture method, variations in the size and shape of collectors, the materials of collectors, and analytical techniques for identification could affect the final results, alongside variations in the sample preparation procedures and sampling times. According to the sensitivity of various analytical techniques for microplastic analysis, the µFTIR technique can detect particles larger than 5–20 µm depending on the resolution and sensitivity of the equipment used. Particles down to 0.5 µm are suited for Raman analysis, with identification for both techniques based on acquired spectra. For optical microscopy analysis—the method used in our study for the microplastic quantification—the detection limit is approximately 1 µm but it is limited in identifying microplastics because only colored microplastics are counted for quantification. Consequently, the number of microplastics in the samples could be underestimated. However, microscopy is easily accessible in any research laboratory and requires less expertise in sampling observations, analysis, spectra processing, and identification, making it a more cost-efficient technique that could be used worldwide for microplastic quantification.

For comparison, we considered reported works that used NILU collectors similar to the ones used in our study or made from PTFE instead of Inox, with optical microscopy for identification at first, and then other passive collectors with optical microscopy or other analytical techniques for identification of MPs and fibers, without considering the sampling period and sample preparation technique.

The optical microscopy analyses of microplastics and fiber pollution over the sampling period reveal significant temporal variability in both the absolute counts and relative proportions across samples. High absolute counts of microplastics in April and May 2023, coupled with high percentages of microplastics compared to fibers, suggest periods of intense microplastic contamination. Conversely, higher fiber percentages during other times highlight the dynamic nature of environmental contamination. The trends suggest potential seasonal or event-driven variations that influence microplastic and fiber prevalence, such as wind speed and precipitation, as shown by the PCA analysis.

In our study, we divided the samples into size fractions of >125 µm, 125–63 µm, 63–25 µm, 25–12 µm, and 12–1.2 µm. The 12–1.2 µm fraction represents MPs with sizes falling within the atmospheric PM_{10} and $PM_{2.5}$ fractions, which are of most concern for human health. Therefore, our methodology allowed us to perform a more detailed study on the proportions of microplastics and the seasonal distribution in the fraction below PM_{10} compared with the entire atmospheric microplastic spectrum. The distribution of fibers by size fraction indicated several critical trends in fiber contamination. Firstly, smaller fibers (12–1.2 µm and 25–12 µm) were more common in the environment. This could be attributed to the breakdown of larger fibers over time or the predominant sources of fiber pollution contributing more to smaller sizes. Secondly, there were considerable fluctuations in fiber counts over time, particularly noticeable in the smaller size fractions. Peaks in fiber counts often coincided with specific dates, suggesting episodic events or seasonal variations in fiber pollution.

The results of the distribution of microplastic particles across various size fractions (>125 µm, 125–63 µm, 63–25 µm, 25–12 µm, and 12–1.2 µm) offered insights into the prevalence and variability of microplastics in different size categories. Overall, the analysis of microplastic particle size fractions reveals several key trends: there is a notable increase in the number of microplastics as the size decreases, particularly in the 25–12 µm fraction, suggesting that smaller microplastics are more common in the environment, likely due to degradation processes breaking down larger plastics over time—the aging of microplastics. Outliers in size fractions highlight the variability in microplastic contamination across different samples, underscoring the importance of considering local environmental factors, sampling methods, and potential contamination sources when analyzing microplastic data. The outliers observed in the >125 µm, 125–63 µm, 63–25 µm, and 25–12 µm fractions suggest that the samples occasionally exhibit exceptionally high levels of microplastic contamination. These could be areas of interest for further investigation to identify and mitigate sources of pollution.

Between the two smallest (25–12 µm and 12–1.2 µm) size fractions examined over time, the results indicate fluctuating levels of microplastic per day and per square meter ($MPs/day/m^2$) contamination. From September 2022 to March 2024, the 25–12 µm size fraction generally exhibited higher counts compared to the 12–1.2 µm fraction, with peaks observed in February 2023 and May 2023. This pattern suggests varying sources and deposition rates of microplastics in the sampled area. Interestingly, some sampling dates, such as December 2022 and January 2023, showed an increase in microplastic counts for the smaller size fraction (12–1.2 µm), indicating potential shifts in distribution and accumulation. The data also highlight specific spikes in size fractions (25–12 and 12–1.2) and in the total microplastic counts across all fractions from 5 mm to 1.2 microns during the sampling campaign. These spikes are not uniform and do not match each other across these fractions, potentially correlating with seasonal variations or local anthropogenic activities.

The wind rose data collected from 29 September 2022 to 5 March 2024 highlight a diverse range of wind directions in the study area, with a predominance of easterly (E), southerly (S), southwesterly (SW), and northerly (N) winds. Notably, easterly winds were the most frequently observed, particularly on 15 February 2023 and 6 February 2024. Southern winds also appeared prominently on various occasions, while northerly and southwesterly winds were less consistent but still notable.

The variability in wind direction observed throughout the study underscores the dynamic nature of local meteorological conditions. This variability has implications for the dispersion of airborne particles, such as microplastics and fibers. The strong positive correlations between northwesterly (NW) and northerly (N) winds with microplastic concentrations suggest that these wind directions are associated with higher levels of microplastics, likely due to their capacity to transport them over longer distances. Conversely, southerly (S) and southeasterly (SE) winds exhibited negative correlations, indicating a potential for these winds to reduce microplastic and fiber concentrations, possibly through mechanisms such as microplastic/fiber deposition or dilution. The absence of significant correlations for winds from the west (W), southwest (SW), and periods with no significant wind (null) suggests that these factors may have a less consistent impact on microplastic levels. The unique occurrence of northeastern (NE) winds on 24 May 2023, with a moderate positive correlation to microplastic concentrations, further emphasizes the complexity of wind-driven microplastic dispersion.

The PCA results reveal distinct patterns in how meteorological factors influence microplastic concentrations. PC1 highlights the importance of precipitation and wind speed, suggesting that these conditions are closely associated with higher microplastic levels. PC4 suggests that microplastic counts represent it directly and are associated with humidity levels, particularly under low-humidity conditions.

In comparison with other studies, a NILU collector was used in the French Pyrenees and reported atmospheric wet and dry deposition, identifying fibers up to ~750 µm long and fragments $\leq$ 300 µm as microplastics [23]. The researchers documented relative

daily counts of 249 fragments, 73 films, and 44 fibers per square meter deposited in the catchment area. These values are lower than our overall averages across all samples, which are 329 MPs/day/m^2 for microplastic particles and 197 fibers/day/m^2 for fibers. This highlights the higher degree of microplastic pollution in urban settlements compared with less urbanized areas, but even so, this can be transported. Another study, using the same collector [24], investigated anthropogenic microfibers > 200 microns in coastal areas of Ireland, observing an average deposition of 80 fibers/m^2/day across four study sites. Regarding Porto's position in Portugal as a coastal city facing the Atlantic Ocean, our study reported higher average concentrations of fibers in the air.

In a recent study in 2024, with the aid of other types of passive collectors at a remote site in the foothills of the Southern Alps of New Zealand, it was reported that atmospheric microplastic deposition fluxes were six times larger during 24-h sampling periods (150 MPs/m^2/day) than during 7-day sampling periods (26 MPs/m^2/day) [25]. The study highlights the influence of sampling frequency and deposition collector design on limiting microplastic particle resuspension, suggesting that studies with different sampling frequencies may have underestimated atmospheric microplastic deposition fluxes. In our study, an ISO-standard sampler specifically designed for deposition sampling was employed. This equipment provides confidence that the collector is optimized for accurately capturing airborne microplastics. By adhering to these ISO standards, we ensure the reliability and consistency of our sampling process, making our data robust and representative of the environmental conditions being studied.

In a German study where sampling was conducted bi-weekly, similar to our approach, a median number of 275.0 MPs/m^2/day was found across all sampling sites. For six specific sampling sites, the daily fallout ranged from 136.5 to 512.0 MPs/m^2/day, which is less compared with ours—where microplastic particles ranged from 26 to 1484 MPs/day/m^2 and fibers from 14 to 646 fibers/day/m^2 [26].

During a nationwide monitoring of atmospheric microplastic (MP) deposition in Spain, conducted across 10 locations in continental Spain and the Canary Islands from spring 2021 to winter 2022, custom-made metal collectors were deployed for one month during each season [27]. The observed MP deposition rates ranged from 5.6 to 78.6 MPs/m^2/day, with higher values recorded in densely populated areas such as Barcelona and Madrid. The median size of MP fragments (equivalent diameter) was 67.7 µm. In comparison, our study found that microplastics ranging from 12 to 63 µm constituted 63% (equivalent media diameter: 66.6 µm) of the sampled microplastic particles. Additionally, the Spanish study showed that fibers dominated the MP composition, representing at least 70% of identified MPs at all locations. In contrast, fibers in our samples ranged from 13% to 68% of the total microplastic and fiber particles, indicating that the choice between point-sampling and continuous-sampling methods should be evaluated more rigorously.

In Portugal, just one study employed passive collection using borosilicate bulk collectors and FTIR analysis for the microplastic quantification of microplastics >50 µm [28], reporting atmospheric fallout ranging from 0 to 459 MPs/m^2/day across monthly sampling, with higher values during the winter months. Despite differences in size ranges, they observed that smaller-sized microplastic particles were the most common, which coincided with our results.

The analysis of recovery rates for PP, PE-HD, ABS, and PES provides insights into the effectiveness of the filtration process used in this study. PP and PE-HD demonstrated high recovery rates, indicating efficient filtration for these polymers. ABS showed a wide range of recovery rates, suggesting room for methodological improvements. However, at the same time, averages for the recovery rates of particulate microplastics PP, PE-HD, and ABS show similar relatively high values, and the overall average for particulate polymers in the range > 125 µm recorded a 75.9% recovery rate. PES exhibited lower recovery rates in both size fractions (>63 µm—34.7% and 63–12 µm—16.4%), highlighting the need for further refinement in the filtration technique for fibrous polymers that would enable

their catchment. In addition, variability in the recovery rates of the polymers related to morphological type was observed.

Deposition collection is a practical, cost-effective, and efficient method for sampling airborne microplastics; however, variations in the collector types, sampling time periods, sample preparation techniques, and analysis methods for air microplastics and fibers need to be carefully evaluated to compare results accurately.

The findings underscore the important role of wind direction in determining the distribution and concentration of microplastics and fibers in the environment. Winds from the northwest and north are associated with increased microplastic/fiber particle concentrations, while winds from the southeast and south appear to reduce them. These insights are crucial for understanding how atmospheric conditions affect the dispersion and accumulation of microplastics, providing a foundation for developing strategies to manage and mitigate their environmental impact.

5. Conclusions

Overall, this study demonstrates that microplastic pollution is widespread and varies considerably across different size fractions (5 mm–125 µm, 125–63 µm, 63–25 µm, 25–12 µm, and 12–1.2 µm) with prevalence of the 25–12 µm range. Our results underscore the dynamic nature of environmental microplastic pollution, with distinct variations observed in all size-fraction categories across different sampling periods. The microplastic concentrations for the total of the fractions varied between 26 and 1484 MPs/day/m^2 (mean 329, median 211), while fiber concentrations varied between 14 and 646 fibers/day/m^2 (mean 197, median 150). The highest peaks were observed in the smallest size fractions: 164 MPs/day/m^2 (12–1.2 µm) on 26 April 2023; and 534 MPs/day/m^2 (25–12 µm) on 10 May 2023. Recovery rates for PP, PE-HD, and ABS particles were verified as high (75.9%), while PES fibers had lower rates (26.5%).

Meteorological factors, like precipitation, wind direction, wind velocity, relative humidity, and temperature influenced microplastic distribution, as confirmed by the PCA analysis. Continuous monitoring is crucial for understanding the temporal dynamics of microplastic and fiber pollution and informing effective mitigation strategies. Future research should focus on identifying variability in the sources and improving sampling and analytical methods, particularly to enhance recovery rates for fibrous polymers. Optimization of these methods is essential for consistent and reliable quantification of environmental microplastics.

Our study underscores the importance of rigorous methodology and repeated microplastic recovery and quantification testing. Further optimization of the filtration process and additional trials are recommended to ensure consistent recovery rates across all polymer types and size fractions.

Supplementary Materials: The following supporting information can be downloaded at: https://www.mdpi.com/article/10.3390/microplastics3040043/s1, Table S1: Recovery rate data for polymers from the filtration sampling procedure analyzed by optical microscopy; Table S2: Data from all air samples for MPs and fibers analyzed by optical microscopy; Table S3: Independent variables: number of microplastics (5mm–1.2 µm) in the samples and variables calculated from meteorological data for PCA analysis for each sampling period; Table S4: Loading (eigenvectors) of variables in four principal components in PCA analysis.

Author Contributions: Conceptualization, Y.L., H.R., L.P.d.S. and J.E.d.S.; writing—original draft preparation, Y.L.; methodology, Y.L., H.R., L.P.d.S., J.E.d.S., D.S.M., R.P.M.S. and I.F.N.; experimental data acquisition, Y.L., D.S.M., R.P.M.S. and I.F.N.; formal analysis, Y.L.; data curation, Y.L.; writing—review and editing, H.R., L.P.d.S. and J.E.d.S.; supervision, H.R., L.P.d.S. and J.E.d.S.; funding acquisition, H.R., L.P.d.S. and J.E.d.S. All authors have read and agreed to the published version of the manuscript.

Funding: The Portuguese "Fundação para a Ciência e Tecnologia" (FCT, Lisbon) is acknowledged for funding the project PTDC/QUI-QFI/2870/2020 as well as the R&D Unit CIQUP (UIDB/00081/2020

and UIDP/00081/2020) and the Associated Laboratory IMS (LA/P/0056/2020). FCT is acknowledged for funding the PhD grant of Yuliya Logvina (2022.14123.BD) and Luís Pinto da Silva acknowledges funding from FCT under the Scientific Employment Stimulus (CEECINST/00069/2021).

Institutional Review Board Statement: Not applicable.

Informed Consent Statement: Not applicable.

Data Availability Statement: The data presented in this study are available on request from the corresponding author.

Conflicts of Interest: The authors declare no conflicts of interest. The funders had no role in the design of the study; in the collection, analyses, or interpretation of data; in the writing of the manuscript; or in the decision to publish the results.

References

1. Li, M.; Wang, Z.; Zhu, L.; Zhu, Y.; Yi, J.; Fu, X. Research Advances on Microplastics Contamination in Terrestrial Geoenvironment: A Review. *Sci. Total Environ.* **2024**, *935*, 173259. [CrossRef] [PubMed]
2. Munyaneza, J.; Jia, Q.; Qaraah, F.A.; Hossain, M.F.; Wu, C.; Zhen, H.; Xiu, G. A Review of Atmospheric Microplastics Pollution: In-Depth Sighting of Sources, Analytical Methods, Physiognomies, Transport and Risks. *Sci. Total Environ.* **2022**, *822*, 153339. [CrossRef] [PubMed]
3. O'Brien, S.; Rauert, C.; Ribeiro, F.; Okoffo, E.D.; Burrows, S.D.; O'Brien, J.W.; Wang, X.; Wright, S.L.; Thomas, K.V. There's Something in the Air: A Review of Sources, Prevalence and Behaviour of Microplastics in the Atmosphere. *Sci. Total Environ.* **2023**, *874*, 162193. [CrossRef] [PubMed]
4. Regulation-2023/2055-EN-EUR-Lex. Available online: https://eur-lex.europa.eu/eli/reg/2023/2055/oj (accessed on 8 July 2024).
5. Regulation-1907/2006-EN-REACH-EUR-Lex. Available online: https://eur-lex.europa.eu/eli/reg/2006/1907/oj (accessed on 8 July 2024).
6. Communication From the Commission to the European Parliament, the Council, the European Economic and Social Committee and the Committee of the Regions Pathway to a Healthy Planet for All EU Action Plan: "Towards Zero Pollution for Air, Water and Soil". 2021. Available online: https://eur-lex.europa.eu/legal-content/EN/TXT/?uri=CELEX:52021DC0400&qid=1623311742827 (accessed on 8 July 2024).
7. Rep. Pallone, F. H.R.1321-114th Congress (2015–2016): Microbead-Free Waters Act of 2015. Available online: https://www.congress.gov/bill/114th-congress/house-bill/1321 (accessed on 8 July 2024).
8. Marine Debris Program. Available online: https://marinedebris.noaa.gov/ (accessed on 8 July 2024).
9. Sen. Sullivan, D. [R-A. S.1982-116th Congress (2019–2020): Save Our Seas 2.0 Act]. Available online: https://www.congress.gov/bill/116th-congress/senate-bill/1982 (accessed on 8 July 2024).
10. Sen. Merkley, J. [D-O. All Info-S.984-117th Congress (2021–2022): Break Free From Plastic Pollution Act of 2021]. Available online: https://www.congress.gov/bill/117th-congress/senate-bill/984/all-info (accessed on 8 July 2024).
11. Zhang, Y.-Q.; Lykaki, M.; Alrajoula, M.T.; Markiewicz, M.; Kraas, C.; Kolbe, S.; Klinkhammer, K.; Rabe, M.; Klauer, R.; Bendt, E.; et al. Microplastics from Textile Origin—Emission and Reduction Measures. *Green Chem.* **2021**, *23*, 5247–5271. [CrossRef]
12. Giechaskiel, B.; Grigoratos, T.; Mathissen, M.; Quik, J.; Tromp, P.; Gustafsson, M.; Franco, V.; Dilara, P. Contribution of Road Vehicle Tyre Wear to Microplastics and Ambient Air Pollution. *Sustainability* **2024**, *16*, 522. [CrossRef]
13. Järlskog, I.; Jaramillo-Vogel, D.; Rausch, J.; Gustafsson, M.; Strömvall, A.-M.; Andersson-Sköld, Y. Concentrations of Tire Wear Microplastics and Other Traffic-Derived Non-Exhaust Particles in the Road Environment. *Environ. Int.* **2022**, *170*, 107618. [CrossRef] [PubMed]
14. Chen, E.-Y.; Lin, K.-T.; Jung, C.-C.; Chang, C.-L.; Chen, C.-Y. Characteristics and Influencing Factors of Airborne Microplastics in Nail Salons. *Sci. Total Environ.* **2022**, *806*, 151472. [CrossRef] [PubMed]
15. Aini, S.A.; Syafiuddin, A.; Kueh, A.B.H. Quantification, Characteristics, and Distribution of Microplastics Released from Waste Burning Furnaces and Their Associated Health Impacts. *Environ. Qual. Manag.* **2023**, *33*, 303–310. [CrossRef]
16. Leonard, J.; El Rassi, L.A.; Samad, M.A.; Prehn, S.; Mohanty, S.K. The Relative Importance of Local Climate and Land Use on the Deposition Rate of Airborne Microplastics on Terrestrial Land. *Atmos. Environ.* **2024**, *318*, 120212. [CrossRef]
17. Wei, L.; Yue, Q.; Chen, G.; Wang, J. Microplastics in Rainwater/Stormwater Environments: Influencing Factors, Sources, Transport, Fate, and Removal Techniques. *TrAC Trends Anal. Chem.* **2023**, *165*, 117147. [CrossRef]
18. Ryan, A.C.; Allen, D.; Allen, S.; Maselli, V.; LeBlanc, A.; Kelleher, L.; Krause, S.; Walker, T.R.; Cohen, M. Transport and Deposition of Ocean-Sourced Microplastic Particles by a North Atlantic Hurricane. *Commun. Earth Environ.* **2023**, *4*, 442. [CrossRef]
19. Haque, F.; Fan, C. Fate of Microplastics under the Influence of Climate Change. *iScience* **2023**, *26*, 107649. [CrossRef] [PubMed]
20. Xiao, S.; Cui, Y.; Brahney, J.; Mahowald, N.M.; Li, Q. Long-Distance Atmospheric Transport of Microplastic Fibres Influenced by Their Shapes. *Nat. Geosci.* **2023**, *16*, 863–870. [CrossRef]
21. Tan, H.; Mong, G.R.; Wong, S.L.; Wong, K.Y.; Sheng, D.D.C.V.; Nyakuma, B.B.; Othman, M.H.D.; Kek, H.Y.; Razis, A.F.A.; Wahab, N.H.A.; et al. Airborne Microplastic/Nanoplastic Research: A Comprehensive Web of Science (WoS) Data-Driven Bibliometric Analysis. *Environ. Sci. Pollut. Res.* **2024**, *31*, 109–126. [CrossRef] [PubMed]

22. Logvina, Y.; Matas, I.M.; Ribeiro, H.; Pinto da Silva, L.; Rodrigues, P.; Leitão, J.; da Silva, J.E. Micro- and Nanoplastics in the Atmosphere: Methodology for Microplastics Size-Fractionation Sampling. *Microplastics* **2024**, *3*, 82–97. [CrossRef]
23. Allen, S.; Allen, D.; Phoenix, V.R.; Le Roux, G.; Durántez Jiménez, P.; Simonneau, A.; Binet, S.; Galop, D. Atmospheric Transport and Deposition of Microplastics in a Remote Mountain Catchment. *Nat. Geosci.* **2019**, *12*, 339–344. [CrossRef]
24. Roblin, B.; Ryan, M.; Vreugdenhil, A.; Aherne, J. Ambient Atmospheric Deposition of Anthropogenic Microfibers and Microplastics on the Western Periphery of Europe (Ireland). *Environ. Sci. Technol.* **2020**, *54*, 11100–11108. [CrossRef] [PubMed]
25. Aves, A.; Ruffell, H.; Evangeliou, N.; Gaw, S.; Revell, L.E. Modelled Sources of Airborne Microplastics Collected at a Remote Southern Hemisphere Site. *Atmos. Environ.* **2024**, *325*, 120437. [CrossRef]
26. Klein, M.; Fischer, E.K. Microplastic Abundance in Atmospheric Deposition within the Metropolitan Area of Hamburg, Germany. *Sci. Total Environ.* **2019**, *685*, 96–103. [CrossRef] [PubMed]
27. Edo, C.; Fernández-Piñas, F.; Leganes, F.; Gómez, M.; Martínez, I.; Herrera, A.; Hernández-Sánchez, C.; González-Sálamo, J.; Borges, J.H.; López-Castellanos, J.; et al. A Nationwide Monitoring of Atmospheric Microplastic Deposition. *Sci. Total Environ.* **2023**, *905*, 166923. [CrossRef] [PubMed]
28. P33_marin-Beltran-et-Al_spq.Pdf. Available online: https://ccmar.ualg.pt/sites/default/files/legacy/p33_marin-beltran-et-al_spq.pdf (accessed on 9 July 2024).

Disclaimer/Publisher's Note: The statements, opinions and data contained in all publications are solely those of the individual author(s) and contributor(s) and not of MDPI and/or the editor(s). MDPI and/or the editor(s) disclaim responsibility for any injury to people or property resulting from any ideas, methods, instructions or products referred to in the content.